18

Computer Simulation of Processes at Electron and Ion Beam Lithography, Part 2: Simulation of Resist Developed Images at Electron and Ion Beam Lithography

Katia Vutova, Elena Koleva and Georgy Mladenov
Institute of Electronics at Bulgarian Academy of Sciences
Bulgaria

1. Introduction

Polymer resists are recording and transfer media in electron, ion and photon lithography. The primary aim of lithography process is mastering of relief image in polymer resist layer. This developed and baked pattern is performed to be transferred to substrate trough either: a) plasma or ion (dry) processes or b) wet chemical etching. The transfer of resist relief image can be realised by ion implantation or by "lift off" of deposited on its top thin film (only deposited in open windows in the resist pattern remains after treatment on a strong solvent - namely acetone or methylene chloride). The use of these various microstructure technologies is to create optical, X-ray, electron or ion masks as well as for direct writing of the desired microstructure on the semiconductor wafers for production of integrated circuits. In the same way the resists are used at mastering the micro-structured elements of micro-devices.

The conventional polymer resist is dissolved in a liquid solvent. Usually the liquid resist is dropped onto the sample, which then spins at 1000 to 6000 rpm to form a smooth and uniform film. Immersion deposition of very thin resist film is also applicable. After that the deposited resist layer is pre-baked to 70-90^{o}C to dry the prepared film.

During exposure with appropriate radiation scission and/or cross-linking of the polymer molecules are observed in the resists. An alternative for more complicated resist as chemically amplified resists (CAR's) is creation of an acid agent (from an acid generator component in the compound of the two- or three- component resists) that changes the dissolving protection of the base resin. In this case there are two bake steps: a) pre-bake performed after the spin-coating, aiming to dry the resist by removing the solvent from the deposited resist layer as well as b) post exposure bake (PEB) – the purpose of which is to cause a thermal catalysis of the chemical reactions amplifying the latent bulk image. The second baking step (PEB) is performed in an oven or on a hot plate. The PEB temperature and time are critical for the resist acid generator modification and for acid diffusion and reduction (degradation losses) as well as its evaporation.

At the end of the transfer process the resist is washed away in a solvent such as acetone or a special resist stripper. Often the strip of the resist is done by reactive ion etching in O_2.

Source: Lithography, Book edited by: Michael Wang,
ISBN 978-953-307-064-3, pp. 656, February 2010, INTECH, Croatia, downloaded from SCIYO.COM

At electron and ion beam lithography (EBL and IBL) the resist profile is created as a result of the development process of exposed latent images, containing resist segments with locally modified solubility. This relief image is produced due to the changes of resist thickness and local removal of resist material up to full opening of the irradiated or the non-irradiated areas (respectively in the case of positive tone or negative tone resists). The type of the used irradiation particles - electron or ion is not important when applying the simulation models to the development process. More detailed knowledge and/or comparison of predicted results with experimental data are needed to obtain correct simulation because of the distinct sensitivity behavior for various material compositions.

2. Sensitivity and contrast of electron and ion resists and their developers

The sensitivity and contrast are base parameters of the resist layers, used in the optical lithography, as well as in EBL and IBL. One can evaluate the sensitivity and the contrast of the resist using the experimental dependence d(D) of the resist thickness d at given initial thickness d_0 and at development time t, after irradiation with an average exposure dose D on an area (namely 100x100 μm) and after development of the exposed latent image. At this approach one evaluates change of the resist thickness d in that area during the development process in a chosen solvent called developer. This change is caused by the mentioned dissolution removal of the exposed or the un-exposed polymer. Variable value is the dose D at chosen energy E of the radiation projectiles as well as at constant development conditions (developer type, time and temperature of development). An example of such curve d(D) is given in Fig.1.

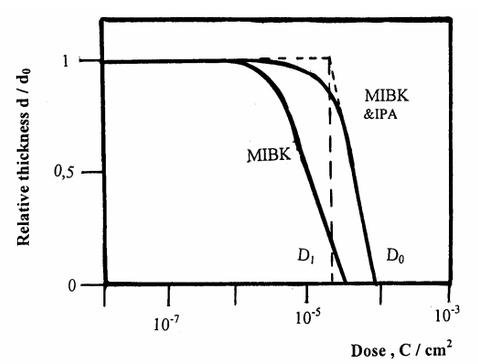

Fig. 1. Dependence of the relative thickness d/d_0 vs. the exposure dose for a positive-tone resist in two developers (MIBK and MIBK& IPA).

The sensitivity of the polymer resist to the radiation is measured as the minimal dose D_0, needed for the development process of the exposed image. This dose is also called dose-to-clear in contrast to the dose, optimized to obtain near to vertical side walls of the developed patterns, usually different than D_o.

In the field of high-resolution lithography it is very important to characterize the edges of the developed profiles in the resist. The contrast parameter γ_d is defined by the dose interval between the initial exposure dose D_1 (at which a start of development in the MIBK&IPA developer can be observed) and the mentioned dose D_0 (for full development of studied resist thickness). These doses are evaluated at increasing doses and chosen time and temperature conditions of the developing process using the bigger dose value of remaining

initial resist thickness d_0 of the utilised resist layer (in the case of positive one) and the minimal dose for full development. Often the curve shown in Fig.1 is called contrast curve.
The values of sensitivity and contrast characteristics in the case of EBL are estimated experimentally in many papers for some average molecular weight of the used resist (measured for example in a.u.) and for a chosen developer. The given data (Brault & Miller, 1980; Karapiperis et al., 1981) presents the sensitivity D_0 and the contrast γ_d in the case of some ion beam resists. Generally, the sensitivity of the polymer resists at the ion exposure is assumed to be higher than at the electron exposure (Brewer 1980; Ryssel et al.,1991). The comparison is not precise due to the different conditions and the peculiarities of the figures of merit used.
The sensitivity and the contrast are described usually as independent properties. Another observed experimental fact is that the solubility rate S of the irradiated spots depends on the used exposure dose D. So at selected (in a set of experiments) resist thickness and development time the curves d(D) are function of the concrete values of the solubility rate S at different exposure doses D.
A definition of another contrast parameter $\gamma_s = (\Delta S/\Delta D)$ as the slope of the solubility rate dependence on the exposure dose S(D) at a given exposure dose (see Fig.2) was accepted. Then can be seen that the parameters γ_s and D_0 for a resist-developer combination are mutually connected (Mladenov & Seyfarth, 1986; Vutova & Mladenov, 2001).
The sensitivity is determined by the radiation efficiency of the couple resist - irradiated particle. The radiation efficiency of the resist g at used kind of radiation can be measured by the mean number of chemical events (chain scission or destruction) per one unit (namely electron volt) of the absorbed energy.
The value of the contrast parameter γ_d for the positive-tone resists and definitions given in Fig.1 can be calculated using the relation:

$$\gamma_d = [\lg (D_1/D_0)]^{-1}, \quad (1)$$

when the removed normalised thickness (namely the ratio $\Delta d/d_0$, where Δd is the removed resist thickness) is equal to 1. In the case of negative-tone resists by analogy:

$$\gamma_d = [\lg (D_0/D_1)]^{-1}, \quad (2)$$

where D_1 and D_0 are the exposure doses at which a start of the development removal (D_1) and the full development, respectively, due to removal of non-irradiated adjacent to exposed pixels (D_0) occurs.
Due to the more smooth transition parts of the d(D) curves observable some times near to the initial dose (D_1) (or near 0% removed irradiated resist thickness for positive resists) and usually at 100% developed image – for negative resists, the rest – straight line sector of d(D) is continued. The doses corresponding to the crossing points of this straight line with the 0 % (or 100%) line is chosen as D_1 and D_0, respectively.

3. Solubility rate dependencies on the exposure dose

The goal of the computer simulation of the processes in EBL and IBL is prediction of the resist profile and the image dimensions of the developed exposed microstructure. During the exposure of the samples, covered by a sensitive to irradiation layer, the local solubility rate of this resist is modified and as a result a developed image as removed and non-

removed areas of the treated resist layer could be observed. Respectively to solubility changes of irradiated areas one could distinguish positive-tone or negative-tone resists. The first important step of the modeling of the resist thickness changes is to transfer the absorbed energy distribution in the resist, caused by exposure, in a distribution of the local solubility (in the case that is also the development) rate. Due to different chemistry composition of utilized resists and to increasing requirements on the exactness of the predicted profiles in various dimension ranges of the developed images (for example- in micron or in sub-micron regions, in sub 0.250 μm or less than 50 nm of the image critical dimensions) the models used in computer simulation of profile dimensions and of its edge are different. The choice of a concrete model and fitting parameters used is the most critical step of this prediction. The integral-circuit-manufacturers use concrete and limited number of resists and any available simulation tool and keep the obtained fitting parameters and applied approximations as confidential as possible.

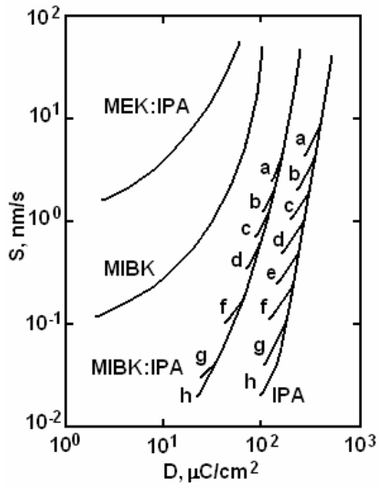

Fig. 2. Dependence of the solubility rate S on the dose D in the case of electron exposure for different developers. The resist thickness is 0.5 μm, the development time is: a - 15 s, b - 30 s, c - 60 s, d - 120 s, e - 240 s, f - 480 s, j - 960 s, h - 1920 s

Fig.2 represents the dependence S(D) in the case of electron exposure of polymethyl methacrylate (PMMA) and the following developers - pure methyl-isobutyl-ketone (MIBK), pure isopropyl alcohol (IPA), MIBK/IPA 1:1 solution and methyl-ethyl-ketone (MEK)/IPA 1:1 solution. This figure shows indirectly that the solubility rate S of the resist is a function of the absorbed energy in the resist for a developer. Experimental investigations also show that S depends on the radiation efficiency of the charged particles in the resist, the resist density and the molecular dispersion. The relation S(D) can be experimentally obtained for a given resist thickness and irradiated particles' energy. The calculated ranges and absorbed energy distribution of the irradiating species can easily convert this dependence in more physically important dependence S(E/V), where E/V is the absorbed energy per one unit resist volume.

In the case of positive-tone resists the solubility rate of the irradiated areas increases while in the case of negative-tone resists - the solubility rate decreases. The radiation affects the density or the number of the modified resist molecules. The changes are weak at lower exposure doses and one can develop the irradiated image at low contrast (and for a very

long developing time). The contrast parameter γ_s can be defined by the slope of the curve S(D) or $S/S_0(D)$. Taking into account that $S=\Delta d/t$, where $\Delta d = (d_0-d)$ is the removed thickness and d_0 is the initial resist thickness, it can be found that $\gamma_s=\gamma_d/(t.d_0)$, i.e. γ_s is proportional to γ_d. In the cases of higher doses (that means - lower sensitivity of the resist) one can obtain a desirable irradiating image for shorter time, that is practical, and usually at higher contrast. This means that one can trade sensitivity for contrast.

The use of a mixture solvent/non-solvent as a developer of electron irradiated polymer (such weak developer is the mixture of MIBK and IPA in the case of PMMA) improves the contrast together with a loss of the sensitivity. In this case it was observed a non-linear behaviour of the solution process (Mladenov & Seyfarth, 1986). In Fig.2 one can see two cases of polymeric layer solution: (i) linear resist solution with a constant solubility rate during development process and (ii) non-linear resist solution with variable solubility rate during the development time. An initial dose from which development begins and an initial solubility rate at every chosen development time take place in the non-linear development of PMMA and a weak solvent is used as a developer. This phenomena is connected to the selectivity of the solution at different molecular weights of the fractions and to the diffusion processes of the developer in the polymer resists. The differences in the observed multi-ciphered dependencies are small and they could be neglected in numerical simulation of the development process in PMMA resist.

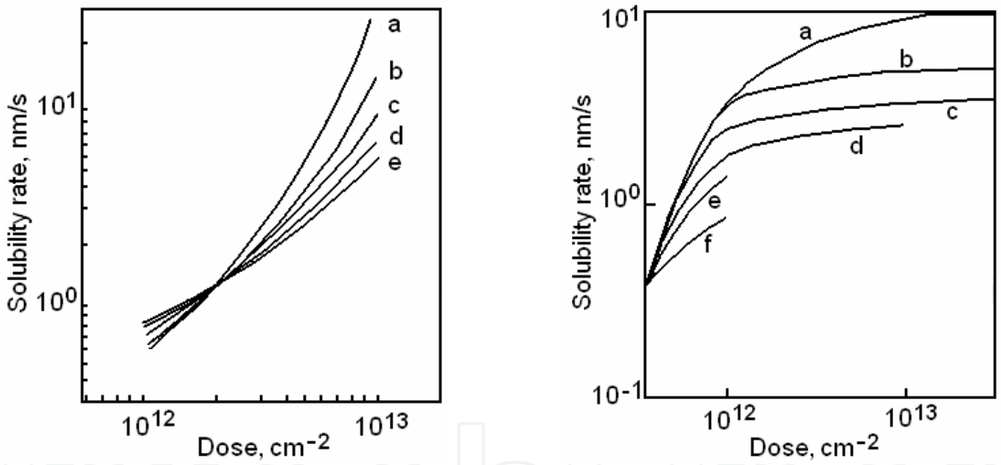

Fig. 3. Solubility rate of PMMA (M=675 000) using MIBK:IPA (1:1) at 20^0 C after exposure with: a) 80 keV He^+: a - 30 s, b - 60 s, c - 90 s, d - 120 s, e - 150 s; and b) 120 keV Ar^+: a - 30 s, b - 60 s, c - 90 s, d - 120 s, e - 150 s, f - 300 s.

In the case of ion exposure process a similar linear or non-linear solution processes were observed pertaining to ion mass (Brault & Miller, 1980; Karapiperis et al., 1981; Vutova & Mladenov, 2001) due to the different radiation ion efficiency to the energy transfer and subsequently, to different latent images. In Fig.3 one can see the non-linear (multi-valued) solubility rate obtained in the case of He^+ (Fig.3a) and Ar^+ (Fig.3b) irradiations of PMMA. A dependence of the contrast on the developing time (and the resist thickness) can be seen. The difference between the electron resist non-linear solution process and ion resist non-linear solution process is connected to the difference of the energy deposition processes in the polymer in both cases. In the case of EBL there is high probability that the electrons will

be more deflected from the initial path (up to back scattering) as well as the created secondary electrons will have high energies. As a result the resist layer up to a distance of a lot of microns from the irradiating point is changed. Differently, the electronic stopping power is responsible for the resist solubility modification in the case of ion exposure with low masses (Mladenov & Emmoth, 1981; Mladenov et al., 1985). This leads up to a distribution of the modified resist pixels (in an order of 100 nm) near and around the ion track. Ion irradiation defects in the polymer layer, caused by nuclear energy losses, can be a reason for the lower solubility rate at high doses as well as the more strong decrease of solubility rate at heavier irradiating ions. Note that in IBL development the increase of the exposure dose causes bigger difference between the development rates for various development times (opposite to PMMA and weak developer case, shown in Fig.2).
As a conclusion it could be noted, that non-linear behavior during the time of development could be expected to be a more general case and probably an important phenomena in the processes of development of the smallest images where more details of the development process are of considerable value. Note that at more complicated processes of solubility modification (in the case of three component resists, chemically amplified resists) the dependencies S(D) are functions of more parameters such as initial photo-acid generator concentration, times and temperature of post exposure bake, various diffusion coefficients etc. At robust process they are constants and S(D) is an approximation that is applicable for the computer simulation.

4. Data for the resists used in the electron beam nanolithography

4.1 PMMA in nanolithography

An organic one-component positive tone resist, which is extensively used in nanolithography, is special grades of polymethyl methacrylate (PMMA) with molecular formula $[CH_2C(CH_3)(CO_2CH_3)]$. The wide use of PMMA is due to the fact that it has high resolution, wide processing latitude, it is easy to handle and forms excellent film. In many papers, a resolution of developed PMMA patterns bellow 10 nm of isolated features and dense array of 30 nm parallel lines at a pitch of 30 nm (periodic grating) is demonstrated. For this aim thin membrane substrates, thick polymer sub-layer or high accelerating electron energy (80-200 keV), ultrasonic assisted development were used (Moreau et al., 1979; Cumming et al., 1996; Hatzakis, 1998; Yasin et al., 2002)
The predominant mechanism of polymer solubility modification in PMMA is chain scission between the carbon atoms changing the molecular weight distribution and decomposition of carbonyl radicals to volatile products. The required irradiation dose is high (as example 50 $\mu C/cm^2$ at 20 keV accelerating electron energy and developer methyl butyl ketone - MIBK). Some co-polymerizing PMMA compounds (with polymethacrylic acid or anhydride) could enhance 2-3 times the PMMA sensitivity (Hatzakis, 1998). The concentration change of the developer (to a mixture of strong dissolving agent and weak or non-solvent agents as iso-propanol (IPA) or water) is a way to improve the contrast (that is important for higher resolution) at decreasing of the solubility (Vutova & Mladenov, 2001; Yasin et al., 2002). Experiments were executed using 400-1000 nm thick PMMA films. In the sub-10 nm region the use of development assisted with ultrasonic agitation, instead the standard puddle development is important (Chen & Ahmed, 1993). This increases the development rate and in this way a lower dose of exposure could be applicable: 6.4 - 7.5 $\mu C/cm^2$ at 20 keV accelerating electron energy (Vutova & Mladenov, 2001) and 200 nm thick PMMA. Rinse in IPA decreases the roughness of the developed lines (Yasin et al., 2004).

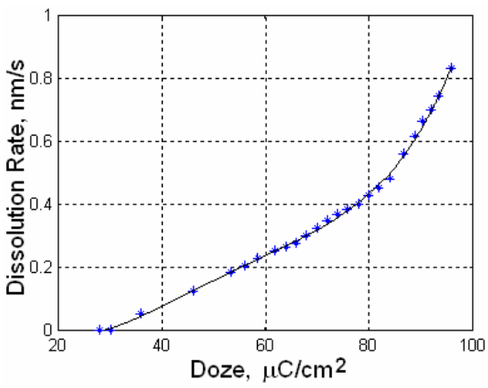

Exposure	electrons	
PMMA	A2	Microchem
Mol. weight	950 000	
Thickness	50 nm	
Substrate	Si	
Developer	MBK:IPA	1:3
Development Time	60 sec	
Developer Temperature	20° C	
PreBake	170° C	30 min oven
E-beam	30 keV	

Fig. 4. Dissolution rate, calculated for PMMA at the given parameters (50nm, 30keV)

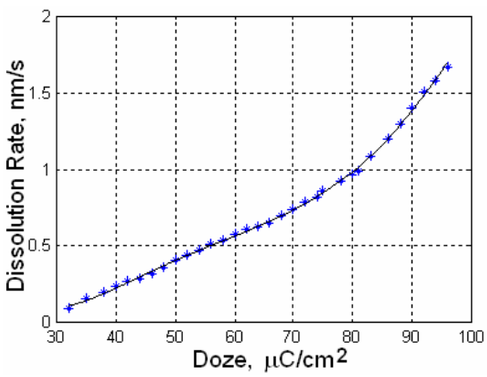

Exposure	electrons	
PMMA	A2	Microchem
Mol.weght	950 000	
Thickness	100 nm	
Substrate	Si	
Developer	MBK:IPA	1:3
Development Time	60 sec	
Developer Temperature	20° C	
PreBake	170° C	30 min oven
E-beam	20 keV	

Fig. 5. Dissolution rate, calculated for PMMA at the given parameters (100nm, 20keV)

Our experience concerning development of thin PMMA films - 100 nm and 50 nm thick films (PMMA with 950 000 Mw, development time 60s, temperature 20° C, developer MIBK:IPA 1:3, substrate Si, Pre-bake 170° C, electron energy from 20 keV to 30 keV) shows a lower contrast in the region of exposure doses from 30 μC/cm² to about 80 μC/cm² and an improved contrast parameter at exposure doses higher than 80 μC/cm² (see Fig.4 and Fig.5). The calculated dissolution rates, using experimentally measured relative changes of resist thickness during development process, at various doses of electron exposure are different for different resist thicknesses (in Fig4 and Fig.5 the energies of the exposure electrons are also different). There A2 means 2% dissolution in Anisole as a solvent.

To check the role of the changed electron energy we calculated the dependence of the absorbed electron energy distribution on the radial distance (from the direction of the initial movement of the beam electrons) using the approach discussed in the Part 1 of this Chapter (Fig.6 and Fig.7). One can see that the back scattered electrons are more widely distributed and have a lower amplitude in the case of a higher accelerated voltage (Fig.6). So the increase of the development rate in that case could be expected at higher exposure doses and this factor could not change the development rate at lower doses. The values of all development rates are higher in the case of thicker resist layer use (Fig.5). This could be explained by the more important role of the modified surface and interface sub-layers of the

resist film, when the used resist layers have thickness equals to or less than 100 nm. In that way, the characteristics of bulk PMMA become less important than modified boundary sub-layers of the resist at nanostructures lithography using PMMA.

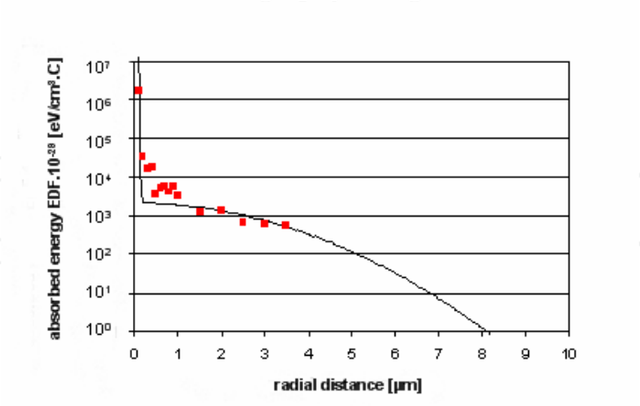

Fig. 6. Absorbed energy on a radial distance, calculated for PMMA 50 nm, 30 keV

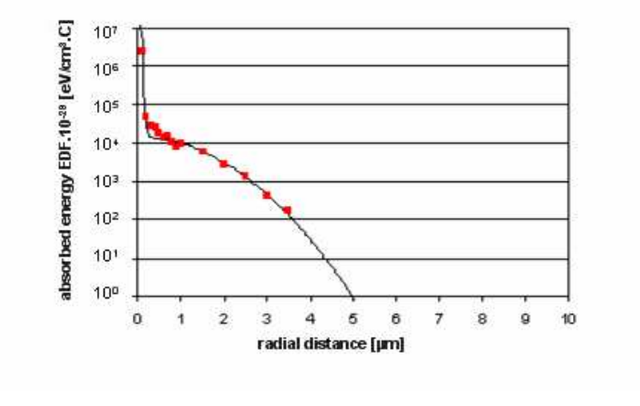

Fig. 7. Absorbed energy on a radial distance, calculated for PMMA 100 nm, 20 keV

For computer simulation of the developed EBL profiles the relations, shown in figures 4 and 5, are estimated using regression models and are given in Table 1.

parameters	equation
PMMA 50nm, 30keV, from 28.8 to 96 μC/cm²	R=0.406085535122903221944181702805- -0.045348294381053866692209145006*D+ +0.0016089764250906957531638749527031*(D²)- -0.000021105769806395996216520396068051*(D³) +0.000000101621149172064510721854383927 4*(D⁴)
PMMA 100nm, 20keV, from 32 to 96 μC/cm²	R = 3.481125084504566373444788611273- -0.340688544477243229401768460987*D+ +0.012485280230500073714286915619175*(D²)- -0.000208081022063644416412397405857 32*(D³)+ +0.000001643336550887558385715408896985*(D⁴)- -0.000000004858414471942250234110958803660 6*(D⁵);

Table 1. Dissolution rates R on the exposure doses D, evaluated using regression models.

4.2 Chemically amplified resists in electron beam nanolithography

To improve the throughput of the exposure process chemically amplified resists (CARs) are developed and used. Due to higher sensitivity the dwell time for imaging of these resists is shorter. Most CARs are a polymer matrix material, the solubility of which is blocked by a component. As an example poly (hydroxysturene) polymer could be blocked with t-butyl carbonyl. In the resist compound a reactive photo-acid generator (PAG) is added and an acid is produced during the electron exposure. After exposure a post exposure thermal bake step is performed to catalyze the reaction between the acid molecules and the protecting group. The de-protecting reaction switches the solubility of the polymer in an aqueous base while regenerating the acid further could amplify the de-protecting reaction. From Table 2 one could see a higher sensitivity at lower exposure doses (less than 100 μC/cm²). Due to that a resist platform for projection electron lithography in nanoelectronics manufacture exists.

Resist	Sensitivity μC/cm²	Resolution nm	Electron energy keV	Film Thickness nm	Paper
SAL605	1,6	50	20	450	Fedynishin et al., 1990
CAMP	60	250	50	300	Novembre&Munzel,1996
ARCH	10	100	50	350	Novembre&Munzel,1996

Table 2. Properties of some CARs in the nano-EBL

In Fig.8 contrast curves of CAMP6 and of two types ARCH CARs are compared with PMMA positive tone one-component nanoresist. The CAMP6 resist has nonlinear behavior during development (Fig.9 – (a) Vutova et al., 2009). The corresponding development rate vs. the dose (Fig.10) is a multi-ciphered dependence. As a result at computer simulation of developed profiles in the resist at the higher exposures doses the resist areas exhibit high dissolution rates and a central zone of the resist has rapid resist removal.

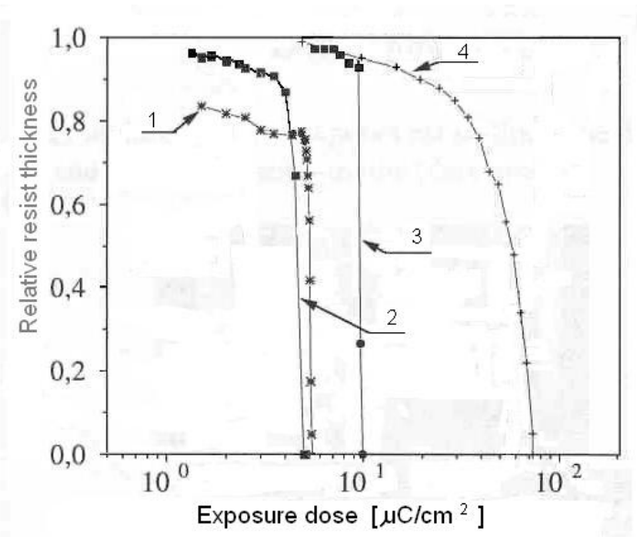

Fig. 8. Contrast curves for: 1- CAMP 6; 2- ARCH2; 3- ARCH; 4- PMMA (bulk) EBL resists

The regression equations for R(D) curves at times of development 15 s and 30 s are shown in Table 4.

Procedure	CAMP	ARCH/ARCH2
Wafer priming in air	HMDS / 60s	HMDS / 60s
Resist spin coating	1 µm, 2379 rpm 0.65 µm, 6000 rpm	1 µm, 2350 rpm 0.7 µm, 6000 rpm
Protective layer spin coating	0.065 µm, 4000 rpm	-
Pre-bake on hot plate in air	120°C, 60s	110°C- 130°C, 60s
EB exposure shaped beam	30keV	30keV shaped beam
Post exposure bake on hot plate in air (immediately after EB exposure)	120°C±2°C, 60s±5%	110°C, 60s
Development (immersion)	OPD262 Developer	OPD262 Developer/OPD4262
Rinse	DI water, 20s	DI water, 20s
Dry spinning in air	1000 rpm, 60s	1000 rpm, 60s
Hard bake on hot plate in air.	120°C, 60s	120°C, 60s

Table 3. Experimental procedures for EBL of CAMP6 and ARCH/ARCH2 resists

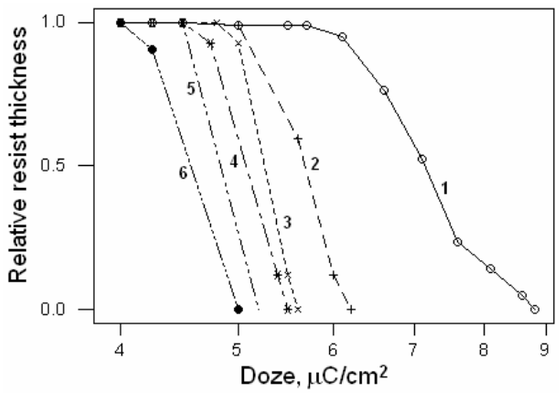

Fig. 9. Contrast curve for 1µm thick CAMP6 CAR at various development times: 1 – 15 s; 2 – 30 s; 3 – 60 s; 4 – 120 s; 5 – 240 s; 6 – 360 s. Thickness loss due to PEB is 23% and d_o = 770 nm

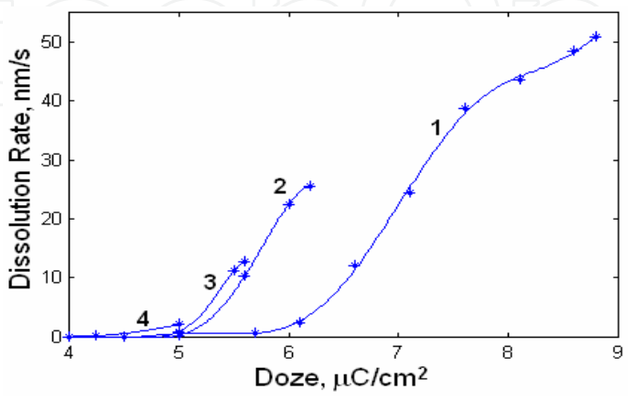

Fig. 10. Experimental characteristics of solubility rate vs dose of electron exposure at various times of development: 1 – 15 s; 2 – 30 s; 3 – 60 s; 4 – 360 s for CAMP6 CAR

Time, dose	Equation
15 s D= 4.5 ÷ 8.8 μC/cm²	R= -102813.405518808108520042676420 35+142167.00666457094955037341868513.D-84825.995315595945739978661788758.D2+28510.530606400510592897424172967.D3-5901.539205985177564395671391522 1.D4+770.16977950614902453894223441137.D5--61.876802541845874295076969973777.D6+2.798542091894069835009907026354.D7--0.0545717270485858077084285932022 56.D8
30 s D=4.95-6.2 μC/cm²	R= 16087.902418081173044563523355944-17028.976699425026854847222308 45.D++7163.363639716611508155801578380 9.D2-1495.84344834865974132417681355 57.D3++154.92193777126500301146841683 68.D4-6.359227822242643634625056659 0707. D5

Table 4. Dissolute rates R on the exposure doses D, evaluated using regression models, for CAMP6 & OPD262 developer (non-linear development process)

4.3 Inorganic EBL nanoresists

After two decades of tests of vacuum deposited inorganic resists, aiming to reach higher resolution due to exhibition of very high contrast and to utilize excellent etch resistance, many inorganic candidates for EBL resists were avoided. The mainly low sensitivity and film quality (pinholes etc) put barriers to its practical development. Recently a spin coated inorganic resist was observed as more attractive – namely the hydrogen silsesquioxane (HSQ) (Namatsu et al., 1998; Namatsu, 2001). The stoichiometric formula of this negative tone resist is $[(HSiO_3)_{2n}]$. The resist is comprised of HSQ resin in a carrier solvent of methylisobutil-ketone. The first use of HSQ was low dielectric constant material for isolation layers in IC fabrication. Its dielectric constant is about 2.6 - 3.0. It provides high thermal stability, good gap-filling and crack free adhesion to metal film surfaces and multilevel interconnects. HSQ is oligomer composed of a caged silsesquioxane along with a linear Si-O network. A standard thermal cure is performed to convert the cages to the highly cross-linked network through reaction in silicon hydride (Si-H) parts of the chains. The same curing reaction could also be accomplished through electron irradiation. It was proposed that Si-H bonds are scissioned during exposure and being converted to silanol (Si-OH) groups in presence of absorbed moisture in the film. These silanol groups are unstable and modified the caged molecules into a linear network. This transition drastically decreases the dissolution rate of matrix in an aqueous solvent performing a negative tone relief pattern. Furthermore HSQ can also be utilized in a bi-layer lithography scheme due to its high etch resistance properties where the patterns are transferred through a sub-layer using a reactive ion etching. Etch resistance of HSQ is excellent. As alkaline developer of HSQ is used usually aqueous solution of tetra methyl ammonium hydroxide (TMAN) - for example 2.38% solution. Resist drying could be optimized effectively by replacing the rinsing liquid with a supercritical fluid (Wahlbrink et al., 2006). Using 30 nm resist and 50 keV electrons a resolution of 6 nm isolated lines and 27 nm period grating were demonstrated (Word et al., 2003). Typical contrast reported for HSQ ranges from 0.55 to 3.2 (Word et al., 2003). The not very good contrast often results in undesired bridging or footing between the developing closely spaced structures. Optimal doses depend upon the beam energy, desired resolution and film thickness. Instead using the mixture of salt and alkali, development in an aqueous mixture of NaOH alkali and NaCl salt enhances the contrast. Contrast values as high as 10 in a 115-nm-thick resist were achieved (Yang & Berggren, 2007). Increasing the temperature

of development to 45°C also increases the contrast and resolution. After baking the resist surface roughness is better than 2 nm over a chip area measured by an atomic force-microscopy.

Thickness nm	Planarization sub-layer nm	Energy keV	Dose μC/cm²	Resolution nm	Paper
20	180	1-3	50	50	Millard et al., 2002
50	Novolack	30		20	Delft et al., 2000
90	-	50	1400	20	Jamieson et al., 2002

Table 5. HSQ characteristics as nano-EBL resist film

From Table 5 one can see the extremely high resolution of HSQ, obtained at cost of higher than in the CARs exposure doses. The contrast and line-wall roughness (line-wide fluctuations) are much lower than the contrast in traditional chain scission PMMA due to the oligomer nature of HSQ. In the references (Namatsu et al., 1998; Grigorescu et al., 2007) the resolution of sub-20 nm features has been also shown.

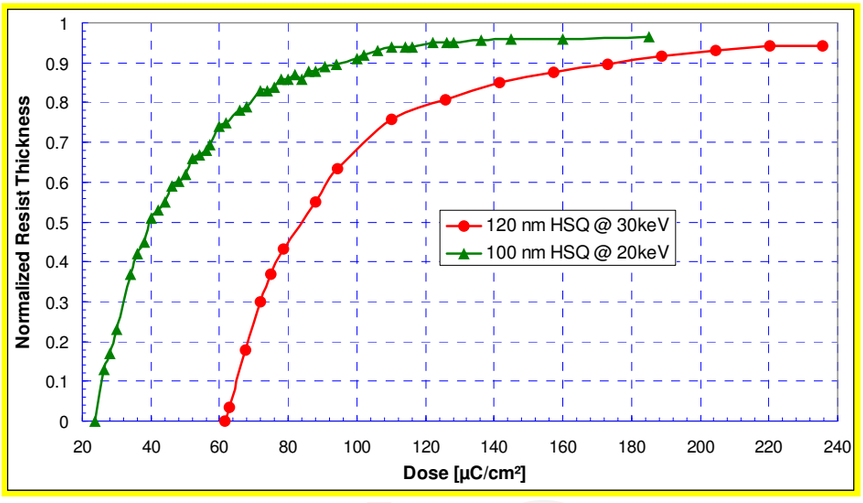

Fig. 11. Resist thickness changes on exposure electron doses at processing parameters - Table 6

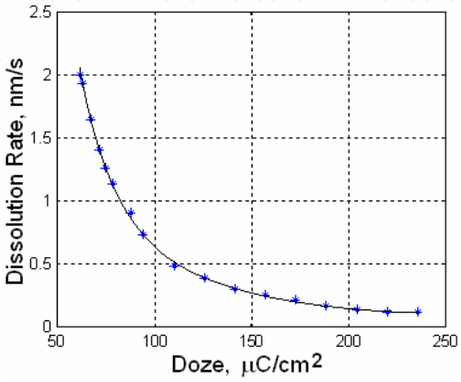

Fig. 12. Dissolution rate calculated for HSQ and parameters in Table 6

The experimental data for HSQ contrast curve (normalized resist thickness vs. exposure dose) is shown in Fig.11. The processing parameters used are given in Table 6. Fig.12 presents the dissolution rate dependencies on the exposure dose, evaluated from the contrast curves shown in Fig.11.

Resist	HSQ FOX-12,Dow Corning
Thickness	120 nm
Substrate	Si
Developer	MF322
Development Time	60 sec
Developer Temperature	20° C
PreBake	120° C, 120 sec oven
E-beam	30 keV
E-beam Current	0.393 A/cm^2

Table 6. Parameters and conditions of HSQ treatment

Evaluated dependencies using regression models of the development rate resist on the exposure dose D for HSQ are given in Table 7. The thickness of the resist film is 120 nm and the accelerating energy of electrons is 30 keV.

parameters	Equation
HSQ 120 nm, 30keV, D=61,5 to 235.8 μC/cm^2	R = exp(5.120539610557917031595849800305 8- -0.11206083135939619970953043371 2*(D) +0.00084258910446202465807879401408491*(D^2)- -0.00000328747319041522259499934957761 76*(D^3)+ +0.00000000497452706273107415528615619072 96*(D^4));

Table 7. Development rate vs. the dose of exposure for HSQ resist and MF322 developer

4.4 Nanocomposite systems in nanolithography

Attempts for optimization of the resist etch characteristics inclusion of nano-particles were tested (Merhari et al., 2002; Ishii et al., 1997), but deeper understanding is still needed. The composition must contain low loading of nano-particles component, such that coagulation and phase segregation are unobserved. The distribution of nano-particles in nano-composite must be homogenous. The studied nanoparticles has been fullerenes and silica (SiO_2) included in CARs. In (Merhari et al., 2002) was been shown, that 7wt % of silica in ZEP520 resulted in a 20-fold reduction in etch rate in oxygen plasma. Resolution in that case was 50 nm. The mechanical stability of nano-images is higher in the case of a wet development. Radiation sensitive metal-organic precursors (Barstow et al., 2002) are tested as other potential high resolution nano-EBL resists.

Assuming the thickness of one-molecule layers as a limiting parameter for a thinnest resist, as an important task for future investigations the authors could point the need for studying the relations between the line width and the minimal resist thickness at various energies (radial energy spread and absorbed energy decrease at decreased resist thickness; there is a situation without losses from the forward penetrating electrons and only back-scattered electrons will modify the resist chains) as well as the role of nanopowder (or by fullerenes) loading of thin resist films at these optimal conditions.

5. Modeling of the resist development

5.1 Background

Various models are presented in the literature, describing the developed resist surface motion and its deformation. Several algorithms have been suggested in the former years (Greeneich, 1974; Dill et al., 1975; Jewett et al., 1977; Hatzakis et al., 1974; Neureuther et al., 1979; Jones & Paraszczak, 1981; Matsuzawa, 1985; Ferguson et al., 1990; Fukuda & Okazaki, 1990; Vutova & Mladenov, 1991; Weiβ et al., 1995; Glezsos et al., 1996) based on these models. The result of the computer simulation is a profile of the developed simple topological patterns, during their formation under particular processing conditions. These models can also be treated as particular cases, with respect to more general study of the profile evolution modeling, during ion etching, film growth and other similar situations, where the anisotropy, the surface tilt influence, the reflection and the secondary deposition make the process rather complex.

One of the first models for the developed contours time evolution described (Greeneich, 1974) is simple, but it is significantly inaccurate. In this model the required development time of each element is determined by summing up the time for reaching its depth and the time of dissolution of its radial distance.

Other authors (Dill et al., 1975; Hatzakis et al., 1974) describe a model, where the resist is partitioned in small elements (cells), coinciding with those, for which the absorbed energy is modeled. Within these elements the solubility rate value is taken to be a constant. Then the element dissolution time is calculated, taking into account the number of the cells' sides that suffer the development process. The profiles are obtained by a subsequent interpolation (on the base of solution times of the various cells).

Two models are described in (Jewett et al., 1977): ray-tracing model and string model. The ray-tracing model is based on the optical analogy of the profile evolution to the light propagation within a medium of variable refractive index. The corresponding value of this index is defined as the ratio of the maximum to the local value of the solubility rate. In the string model the simulated profile is presented by straight line segments, whose ends advance along the angle bisector of the two adjoining segments according to the local value of the solubility rate. During the modeling process, the segments are kept roughly equal in length by adding points in regions of expansion and removing points in regions of contractions. The majority of the mentioned published simulation models describe the solution and removal of the resist material as a surface process, that take place on the interface solid resist/liquid developer. We will see that when one tries to simulate resist material removal during nanolithography processing, this assumption becomes too rough.

A number of problems appear when trying to use in practice the described models. Some of them are listed bellow:

- most often, part of the model details (the calculation of the absorbed energy in the resist, the relation absorbed energy/solubility rate, the profile evolution algorithm etc.) are not presented in the papers and that's why the models are practically unusable;
- different experimental data has been used for the solubility rate characterization (usually it is not mentioned that the measured solubility rate is the average value and the range of calculating this mean is not defined);
- in order to obtain a final result of an appropriate accuracy, even the modeling of simple elements requires a proper choice of a fine grid, which leads to higher costs of the

simulation. This explains why only in refs. (Jones & Paraszczak, 1981; Matsuzawa, 1985) numerical calculations are carried out for 3D profiles of simple developed patterns.

There are few development models (Jones & Paraszczak, 1981; Matsuzawa, 1985; Ferguson et al., 1990; Fukuda & Okazaki, 1990; Weiβ et al., 1995) based on knowledge of 3D concentration distribution of a dissolution inhibitor in the resist layer after the exposure (including the delay and post exposure baking in the case of CAR's). The conversion of the resist material during electron irradiation (catalytic decomposition or creation of an acid from the acid generator) and the loss or diffusion of this inhibitor need a large number of input parameters and a simple model can be found in (Neureuther et al., 1979). But in this approach (solubility rate versus dissolution inhibitor concentration) the evaluation or experimental measuring of this inhibitor concentration is an open question.

Despite the common nature of the listed models, the development of a particular algorithm and the corresponding computer program need the solution of several problems such as: (i) the creation of developed resist profile with a slope in one of the two possible directions with respect to the initial surface normal; (ii) the particularities of the profile evolution at the points of smoothness discontinuity, due to the model assumptions; (iii) the graphical interpretation of the surfaces; (iv) the appropriate links of the program units, forming the whole working package.

In our model of development process (Mladenov et al., 1987; Vutova & Mladenov, 1991; Vutova & Mladenov, 1994; Mladenov & Vutova, 2002, Vutova & Mladenov, 2008; (a) Vutova et al., 2009; (b) Vutova et al., 2009) we assume that the resist is homogeneous enough and the development process is isotropic. To increase the accuracy of the end point position of the evolving point trajectory at a given time smaller time steps are used. The main features of the model are: (1) the motion of the evolving point takes place along the normal to the corresponding profile; (2) the space modification of the absorbed energy distribution is also taken into account; (3) in our model, we use a cubic spline in the 2D case and a bicubic spline in the 3D case to describe the developed profiles; (4) an original procedure is applied for the profile discretization to increase the contour accuracy. There is a reduction of the evolving points number (i.e. density) in the profile regions, where the normal tilt is kept close to the initial profile slope, and increasing the evolving points number in the profile regions, where a maximum change of the slope is observed.

5.2 Simulation of 2D developed contours of the resist profile at a linear development process

Our model (applied for a positive resist) can be described by the following steps:

Step 1. In order to trace the development contours in the resist plane a Cartesian coordinate system is introduced. The axis Ox is at the resist surface, and Oz is in its depth. A finite number of points on the resist surface is chosen, where the evolution of the time development contour will be traced.

Step 2. The spatial distribution of the adsorbed energy E_i per unit of the resist volume V and at used dose D is calculated (see part 2 and 3). The subscript i denotes the number of the points from the examined contour.

Step 3. The change of the resist solubility that is determined from the values of the absorbed energy, results in changes of the polymer molecular weight. That is why during this step, the value of the local deposited energy density $D_i.(dE/d\xi)_i$ is transformed after radiation into the new molecular weight values of the resist in vicinity of the point i, using the relation (Greeneich, 1974):

$$\frac{1}{\overline{M_{fi}}} = \frac{1}{\overline{M_n}} + \frac{g.D_i}{\rho.N_A}.\left(\frac{dE}{d\xi}\right)_i , \tag{3}$$

where $\overline{M_n}$ is the original average molecular weight; $\overline{M_{fi}}$ is the fragment average molecular weight; g is the radiation efficiency value; ρ is the polymer mass density; N_A is the Avogadro's number and D is the average exposure dose of a single spot.

The movement of the point is traced along the normal to the initial contour (for instance z=0). Its velocity is calculated by converting the molecular weight values $\overline{M_n}$ into solubility rate values S_i , using the empirical formula:

$$S = R_0 + B \,/\, \overline{M_{fi}}^{A} , \tag{4}$$

and the relation (3). The development time (i.e. the time of movement of the evolving point along the normal) must be sufficiently small. Criteria for this are the number of the required profiles, the accuracy of their modelling as well as the missing intersection of adjacent evolving point trajectories. Using this way, one can obtain the coordinates of the points, defining the new contour.

Step 4. N-cubic splines are build. So the new developed profile is described on the basis of the obtained points set:

$$z = C.z_i + D.z_{i+1} + G.z_i'' + H.z_{i+1}'' , \tag{5}$$

where

$$C = \frac{x_{i+1} - x}{x_{i+1} - x_i} ; \qquad D = 1 - C ; \qquad G = \frac{1}{6}\left(C^3 - C\right).\left(x_{i+1} - x_i\right)^2 \tag{6}$$

and

$$H = \frac{1}{6}.\left(D^3 - D\right).\left(x_{i+1} - x_i\right)^2 . \tag{7}$$

Here z'' is the second derivative of the z function.

Step 5. The angle α between every two evolving points is calculated. Its value is compared to π/2. If the two values are close enough, then the modification of the development contour between the two points is insignificantly small. In this case the point (x_{i+1}, z_{i+1}) is not considered in the subsequent calculation. If this angle is small, i.e. there is a significant profile modification a new point $x = \frac{x_i + x_{i+1}}{2}$ between these two points is introduced, in order to estimate more precisely the profile change in this area. This test was done for all the evolving points. Then the second step is applied again until a given development time is reached.

In the case of negative resists in Eq.(4) the power index A is negative and one can use the relation:

$$S = S_0.\left[C_0 + \frac{2g.D}{e.\rho.N_A}.\left(\frac{dE}{d\xi}\right)\right]^{-A} , \tag{8}$$

where S_0, g and A are parameters, the physical meaning of which are: the initial solubility rate at the resist surface ($S_0.C_n^{-A}$), g(cl) is the radiation efficiency for cross-linking defined as a number of the chemical joining per 1 eV absorbed energy, and A is the power index of the solubility rate decrease.

Here it is also assumed that there an associated molecule at bonding two polymer molecules by one cross linking is created. The constant C_n is connected to the average initial molecular weight of the resist $\overline{M_n}$. The exposure dose is in [C.cm^{-2}].

5.3 Peculiarities of ion lithography 2D development model

A formula that gives the relationship between the molecular weight of the resist after radiation $\overline{M_{fi}}$, the original molecular weight $\overline{M_n}$ and the exposure parameters can be found in a similar way to the case of electron exposure. In the case of ion exposure of the resist the $\overline{M_{fi}}$ can be represented as a function of the electronic and nuclear energies:

$$\frac{1}{\overline{M_{fi}}} = \frac{1}{\overline{M_n}} + \frac{\left[g_{el} \cdot \left(dE / d\xi \right)_{el} + g_n \cdot \left(dE / d\xi \right)_n \right] . D}{\rho . N_A} , \tag{9}$$

where g_{el} and g_n are the corresponding radiation efficiencies for the two component of the absorbed energies. If we define:

$$g = g_{el} + g_n \cdot \frac{\left(dE / d\xi \right)_n}{\left(dE / d\xi \right)_{el}} , \tag{10}$$

then Eq.(9) can be written as Eq.(3) and the solubility rate S is given by Eq.(4) that were used in the case of electron exposure.

In the studied case of ion beam exposure one can assume that the particular development characteristics R_o, B and A in Eq.(8) have the same values as in the case of electron lithography. This assumption is based on the dominance of the electronic energy losses. When the value of the ratio of the nuclear to electronic stopping powers in Eq.(10) is negligibly small, g=g_{el}. This is true in the case of light ions incident on a polymer in ion implantation energy region (tens hundreds keV) and for all ions at higher energies.

5.4 Three dimensional model for the simulation of the development profile

Introducing the coordinates of the exposed pattern (for example a rectangle) one can examine the evolution of the resist surface, using a finite set of points, as in the case of 2D case. Similarly, we obtain a new set of points and approximate the new surface using a bicubic spline. Let x_1, x_2, x_3….x_i….x_m and y_1, y_2, ….y_j….y_n are a set of points with corresponding function values $z_{ij} = f(x_i, y_j)$ where i = 1, 2 ,…m, j = 1, 2,…,n. The aim is to estimate the function f at some non-tabulated point (x*, y*) by interpolation procedure. More precisely, if:

$$x_i \le x^* \le x_{i+1} \qquad y_j \le y^* \le y_{j+1} \tag{11}$$

then the next expression gives the necessary values:

$$f(x',y') = \sum_{k=1}^{4}\sum_{l=1}^{4} C_{k,l}.t^{k-1}.u^{l-1}\,, \tag{12}$$

where $C_{k,l}$, k, l = 1, 2, 3, 4 are constant values. The formulas that obtain the sum from the functions and derivative values are just a complicated linear transformation with coefficients which, having been determined once, can be tabulated (Abramowitz & Stegun, 1964; Dahlquist & Bjorck, 1974). Then:

$$t = \frac{x' - x_i}{x_{i+1} - x_i} \quad \text{and} \quad u = \frac{y'' - y_j}{y_{j+1} - y_j}. \tag{13}$$

After the calculation of the new development profile, the step is repeated for the next time interval. The process stops when a given development time is reached.

5.5 Peculiarities of the simulation of the development profile in CARs - a simplification

As it was shown, in the case of PMMA, as typical example of the one-component resists, the conversion of the absorbed energy distribution in the resist to the solubility rate is based on the radiation modification of the polymer molecular weight in studied point of the resist. At chosen couple resist – developer, conditions of development, resist initial molecular weight, exposure dose and radiation yield, a definitive development rate could be estimated. The dissolution rate of the unexposed resist at these conditions is another parameter used in the simulation. Often the changes of the absorbed energy density distribution on the resist depth are neglected and only its radial (lateral) distribution is used at the simulation. Two types of the resist solubility were distinguished: linear and nonlinear solutions. Reasons for these phenomena are various: the role of an interface layer with solubility rate other than one of the bulk resist material, time dependence of the developer penetration into the solid resist, the role of the nuclear energy losses that deteriorate the polymer structure at ion modification of the resist material etc.

Then the resist removal in a linear development case is simulated as a movement of the interface between the solid polymer and the liquid developer. The developer – resist interface is a function of the time of development. For a short developing time each evaluating point from the moving development contour (or plane in the case of 3D simulation) advances along the normal to the profile with its local solubility rate. A procedure to increase the contour (plane) accuracy by increasing the evaluating point numbers in the parts with significant curvature is applied.

In the case of chemically amplified resists (CARs) there are two or three polymer components one of which is a radiation active component (RAC). During exposure of RAC the absorbed energy effect is a generation of a radiation product. Additionally a diffusion of that radiation product takes place during a thermal process, called post-exposure bake (PEB) applied in this case. In the CARs this radiation product (an acid) works as a catalytic agent and modifies the base component solubility rate. The models of the conversion of the solubility rate through the RAC concentration and the solubility rate modification products are described (Dill et al., 1975; Kim et al., 1984; Ferguson et al., 1990; Glezos et al., 1996).

In these models various descriptions of the diffusion and loss of the catalytic species (acid) and of the kinetics of the de-protection (switching resist solubility) reaction are used. The

surface changes of the development rate are the reason for other problems. Due to the complicated processing steps and the need of unknown numerical data that describes the reaction kinetics, the published models for simulation of CARs development are not exact. Some models for simulation of the developed resist profiles in CARs consist of models of coupling between diffusion and kinetic reactions; other models describe nonlinear or linear diffusion; there are also various development-rate models (Fedynyshyn et al., 1990; Ferguson et al., 1990). Surface changes (retardation or increase) of the development rate is evaluated using depth dependencies of the resist solubility rate during development (Kishkovich et al., 1999; Vutova & Mladenov, 2001). The processes of resist de-protection and resist removal show threshold or strongly nonlinear behaviour not understood exactly and described quantitatively. Due to that, the choice of a suitable overall lithography simulation model for the concrete resist-developer pair and alternating processing conditions is difficult. Due to many reasons, final experimental calibration of the model parameter set used in such a simulation is needed (Byers et al., 2002; Yen, 2002; Sekiguchi et al., 2001). Some reasons are the following: (i) variations of resist-developer pair and development conditions; (ii) different values of PEB times and temperatures; (iii) different procedures of the experimental parameter extraction; (iv) parameter values that depend on geometry factors; (v) batch-to-batch variations between the resist material characteristics.
A question ((a) Vutova et al., 2009) arises: whether to evaluate each reaction quantitatively, using experimental and theoretic values of too many factors, especially collected in an academic way, or to build one simplified model based on the existing simple experimental calibration procedure. In this model for simulation of development process only main steps could be used: (i) calculation of the absorbed energy distribution in the resist after exposure, (ii) application of experimental solubility rate as a function of the exposure dose and the time of development (multi-ciphered experimental dependencies of the solubility rate on the exposure dose) for approximation of the local development rates in the exposed resist, (iii) application of the procedures for simulation of the developed contour (plane) movement for small time intervals ((a) Vutova et al., 2009; (b) Vutova et al., 2009) in a time dependent calculation scheme. In this way the number of experiments for determining the quantities, relevant for simulation of the development kinetics of the resist profile at a concrete resist-developer system and chosen processing parameters and conditions is minimized.
This simplified model was applied for resist profile simulation in CAMP6 resist. During the development process, the line edge roughness is changed in various phases. Results are shown in Fig.23 below.

6. Calculated developed profiles at EBL and IBL

We assume that our exposed pattern is a 3.1 x 8.1μm^2 rectangle and that the electron beam has an energy of 20 keV and has Gaussian distribution. The results of the calculated contours, characterising the development profile, are obtained in the plane, that contains the line which bisects the longer sides of the rectangle and is perpendicular to the resist surface.
We investigate the modification of the time development contours (at every 1 minute of the solubility process), starting from the surface (Fig.13). Fig.13(a) shows the development profile contours in the chosen cross section. The dose is 1.4x10^{-4} C/cm^2 and the developer is a 1:3 solution of MIBK and IPA. The profile contours in the case of the more powerful developer MIBK are shown in Fig.13(b). In this case we observed an acceleration of the process and a very large difference between the exposed and the developed images.

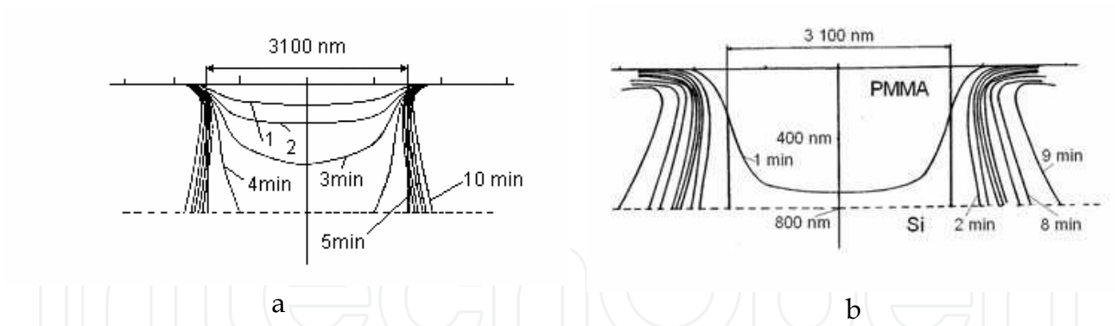

a b

Fig. 13. Time evolution of the cross sectional profiles for a rectangular exposure by electrons of 20 keV at a dose of 1.4×10^{-4} C/cm^2. (a) Development using standard developer which is 1:3 solution of MIBK and IPA; (b) development using MIBK solvent. Resist is PMMA of 800 nm thickness, on Si.

A general test pattern is shown in Fig.14. The structure consist 4 rectangles 1000x1000 nm^2 and a line between them, the width of which is 200 nm. The 3D profile obtained by computer simulation using this test pattern and shown in Fig.15 represents the developed gap surface at a dose of 2×10^{-7} C cm^{-2}. The beam is 60 keV H^+ and the development time is 0.25 min.

Fig.16 shows the shapes of the developed central lines of structure created by exposure of a layout, consisting many 250 nm parallel lines spaced by 250 nm at a dose of 250 μC/cm^2, yield - 0.01, development time – 45 s. The developed line width is 330 nm. The resist used is 400 nm PMMA on Si and the e-beam energy is 50 keV.

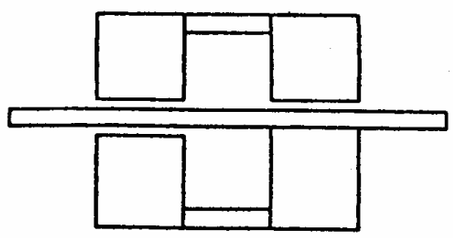

Fig. 14. Two-dimensional pattern for illustration purposes. All small gaps are 100 nm

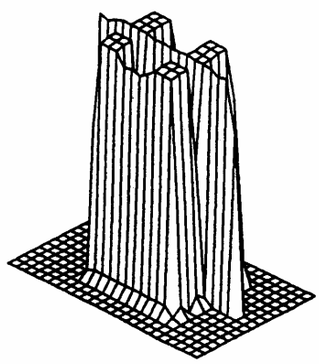

Fig. 15. Computer simulation results for a developed surface using 1:3 solution of MIBK and IPA, applying the test pattern shown in Fig.14.

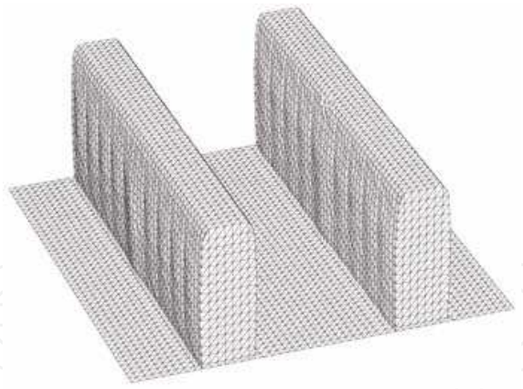

Fig. 16. Part of the 3D resist profile, created by EBL (only the central part of the two parallel lines, situated in the center of the exposed and developed structure, is shown)

Using our computer program for mathematical modeling in IBL, we are able to predict results that can be expected under chosen technology conditions and to learn more features concerning IBL in the region below 100 nm. Some simulation results in the case of ion beam exposure (He^+ ions with energy 100 keV) and development of ion sensitive resist (the exposed resist is 400 nm thick PMMA and the radiation yield is 0.05 eV^{-1}) are presented.
Fig.17 presents 2D simulated resist profile for a line developed in PMMA resist after exposure with 100 keV He^+ ion beam (the image width is 30 nm). In a series of simulations of IBL, the calculated EDF(r) function (see Part 1 of the Chapter) of the absorbed energy for concrete ions was incorporated into the SELID tool. The beam width is presented by the white band in the black mask on the top of the shown structure in Figs.17-19 (the substrate is not shown, the resist layer and the symbolic black mask, added virtually, are indicated on these figures). The developed line width, seen in Fig.17, is 101 nm at the top of the resist layer. This width is 106 nm at the Si substrate while it is 96 nm at the narrowest part of the developed line cross section. This extension of the developed line width is similar to the internal proximity effect obtainable at electron lithography. The resist thickness loss during the concrete development process is 7.1%.
In Fig.18, simulation results are provided for three 30 nm lines exposed with various ion doses. One can see the change of the developed profile shapes when changing the exposure dose. The calculated resist thickness loss is 7.3% at these development conditions. Central line is not developed enough and the optimal, from point of view of obtaining near to vertical side walls of the developed line (trench), is the regime at x= -1 μm.
In the case of IBL of narrow parallel lines, the difference between the width of the exposed and developed lines is also seen, nevertheless the absence of external proximity effect at ion exposure. This case is shown in Fig.19, where Fig.19a presents 2D simulation and Fig.19b presents the result of 3D simulated profile of the resist.

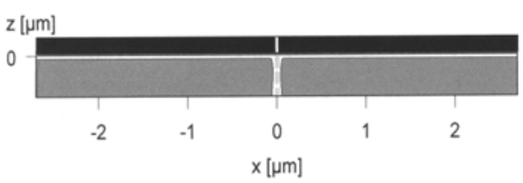

Fig. 17. Simulated resist profiles in the case of 30 nm wide isolated long line at a dose of 0.35 μC/cm^2, 400 nm thick PMMA on silicon, the development time is 5 min

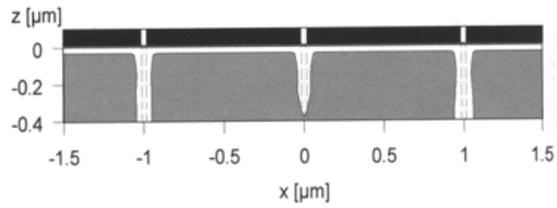

Fig. 18. Simulated resist profiles in the case of EBL of three lines for different exposure doses: 0.325 μC/cm² for the line at x=-1 μm; 0.25 μC/cm² for the line in the center of the figure and 0.4 μC/cm² for the line at x=1 μm

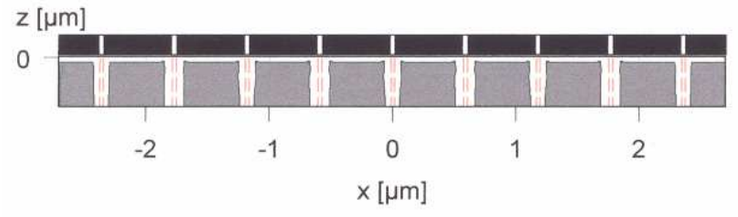

a)

b)

Fig. 19. Simulated resist profiles for nine 30 nm wide long parallel lines spaced by 560 nm after exposure with 100 keV He^+ ion beam. The resist used is 400 nm thick PMMA on Si : a) 2D profile of developed lines; b) 3D resist developed profiles of the exposed parallel lines

A comparison of the same microstructure elements exposed by 100 keV He ions and by electrons is presented in Figs.20-21. The main difference, due to the proximity effect, observable in the case of electron lithography, is that the distance between the line and the squares is 635 nm (Fig.20), while it is 185 nm in the case of IBL (Fig.21). These distances were obtained aiming to minimize it, keeping elements of the structure well different from one another.

Fig. 20. Simulated 3D resist profiles for a layout consisting one 30 nm wide line and four 800 x 800 nm² squares at 50 keV e-beam

Fig. 21. Simulated 3D resist profiles for the layout in Fig.20 after exposure with 100 keV He^+ ion beam

In Fig.20 the influence of the proximity effect on the final result of the whole EB lithographic process is presented - after exposure and development of 30 nm wide central line situated between four 800 x 800 nm^2 squares, the developed line width is 410 nm due to the exposure of the line and absorbed energy added from the squares in the periphery of the exposed central line. In the case of IBL lack of proximity effect is demonstrated and it is important advantage over EBL.

In the case of CARs a time dependent (and multi-ciphered) characteristics were observed (Figs.9-10) due to more detailed study. The developed resist profiles are a result of the developer penetration, volume removal of polymer molecule segments and more complicated chemical and physical changes in the resist than ones in approximation of the developer-resist interface as a simple liquid to solid one.

Fig.22 shows experimentally observed shapes and profile evolution of the 0.5 μm exposed single line in CAR CAMP6. The central part of the line is removed at the beginning and then the resist removal of the line walls widens the trench and vertical side-walls of the developed line (trench) can be observed at higher values of the development time.

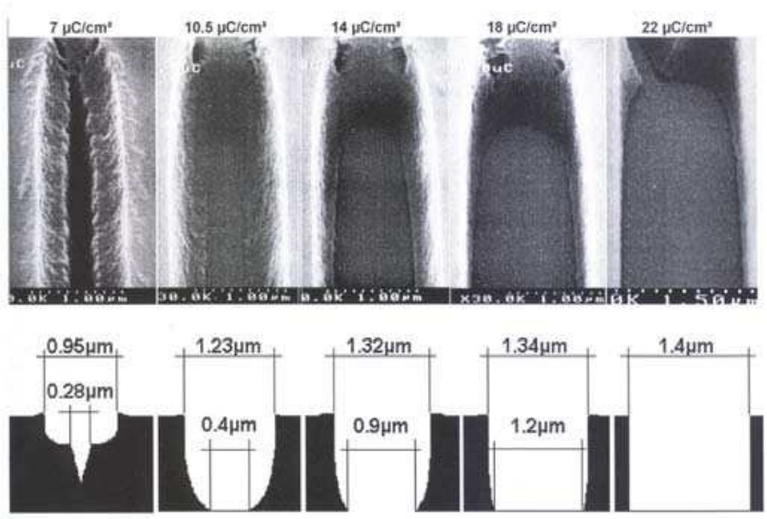

Fig. 22. SEM micrographs (first row) and the corresponding experimental cross-section shapes (second row) of the profile evolution at various exposure doses when 500 nm single lines in 1700-nm-thick (initial resist thickness) CAMP6 (OCG) are exposed.

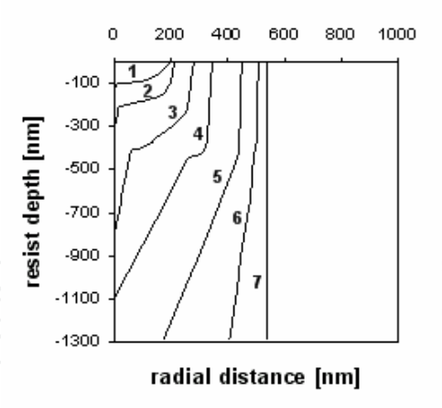

Fig. 23. Simulated development profiles of an isolated 500-nm line created in CAMP6 resist film on Si for different times of development: 1 – 17 s; 2 – 19 s; 3 – 21 s, 4 – 22, 5 – 23 s, 6 – 25 s and 7 – 27 s (half the developed profiles are shown). The developer is OPD-262.

Fig. 23 shows the time evolution of the simulated development profiles for a line in CAMP6 chemically amplified resist using OPD-262 developer. The developed profiles are obtained by computer simulation for the conditions in Fig.22: a single line with a 500 nm width in 1.7 μm thick CAMP6 (initial resist thickness) deposited on Si, the incident electron energy is 30 keV, the beam diameter is 500 nm. From the initial resist thickness of 1.7 μm the remaining thickness was 1.3 μm due to a resist-film thickness loss of non-exposed areas after PEB and development. Higher dissolution rates in the zones with applied higher exposure doses lead to creating a central region of the exposed structure with a rapid removal of the resist. The generated central profile fragment has nearly vertical walls and bottom, which come very quickly to the interface resist/silicon substrate. The resist profiles calculated using our model - curves 3 and 4 (Fig.23) - are in qualitative agreement with the first experimental resist profile, presented in Fig.22 (second row). This resist profile is then extended towards the periphery of the developing structure, obeying the necessary delay time at the boundaries of the different zones. The next profiles – curves 5, 6, and 7 (Fig.23) – with almost vertical walls correspond qualitatively to the experimentally obtained shapes of the rest of the developed resist profiles (Fig.22, second row).

7. Conclusion

In the current work the main steps of the development models for EBL and IBL and their peculiarities are shortly described and discussed. Using the simulation tools the effects of irradiated particles – electrons and ions, exposure dose, dense patterns and nature and characteristics of the development process are discussed in order to extract the necessary values of regime for high resolution patterning. From the obtained results it is seen that the developed algorithms and created new or improved commercial computer tools describe adequately the processes during the resist development at EBL and IBL. The created simulation tools permit to predict with good accuracy the critical dimensions and profiles of the developed pattern. The simulations of IBL structures demonstrate the potential of ion lithography to be considered as one of the main competitors for further improvement of fabrication performance of the new generations of nano-electronic devices.

8. References

Abramowitz, M. & Stegun, L.A. (1964). *Handbook of Mathematical Functions*, Applied Mathematics Series, vol.55

Barstow, S.J.; Jeyakumar, A. & Henderson, C.L. (2002). Direct photo-patterning of metal oxide structures using photo-sensitive metal-organics precursor films, *Proceed. SPIE-Emerging Lithographic Technologies* VI, 421-430, ISSN 0167-9317

Brault, R.G. & Miller, L.J. (1980). Sensitivity and contrast of some proton-beam resists. P*olymer Engineering and Science,* 20 (16), 1064-1068, ISSN 0032-3888

Brewer, G. (1980). *Electron Beam Technology in Microelectron. Fabrication*. Academic Press, N.Y

Byers, J.; Mack, C.; Huang, R. & Jug, S. (2002). Automatic calibration of lithography simulation parameters using multiple data sets, *Microelectronic Engineering*, 61-62, 89-95, ISSN 0167-9317

Chen, W. & Ahmed, H. (1993). Fabrication of 5–7 nm wide etched lines in silicon using 100 keV EB lithography and polymethylmethacrylate resist*, Applied Physics Letters,* 62 (12), 1499-1501, ISSN 1077-3118

Cumming, D.R.S.; Thomas, S.; Weaver J.M.R. & Beaumont, S.P. (1996). 3 nm NiCr wires made using EBL and PMMA resist, *Microel. Eng.* 30 (1-4), 423-425, ISSN 0167-9317

Dahlquist G. & Bjorck A. (1974). *Numerical methods*, v.7, 7.

Delft, F.C van.; Weterings, J.P.; Langen-Suurling, A.K. & Rumijn, H. (2000). HSQ novolac bilayer resist for high aspect rathio nanoscale EBL, *Journal Vac.Sci.Technol*.B, 18 (6) 3419-3423, ISSN 1071-1023

Dill, F.H.; Neureuther, A.R.; Tuttle, J.A. & Walker, E.J. (1975). Modelling of projection printing of positive photoresists, *IEEE Trans. on Electron Devices*, ED-22 , 456-464, ISSN 0018-9383

Fedynyshin, T.; Cronin, M.F.; Poly, L.C. & Konde, C. (1990). Process optimization of the advanced negative EB resist SAL 605, *J.Vac.Sci.Technol*,.B, 8(6), 1454-1460, ISSN 0734-211X

Ferguson, R.A, Hutchingson, J., Spence, C.A. & Neureuther A. R. (1990). Modeling and simulation of a deep UV acid hardening resist, *J.Vac.Sci.Technol.* B, 8 (6), 1423-1427, ISSN 0734-211X

Fukuda, H. & Okazaki S. (1990). Kinetic model and simulation for chemical amplification resists, *Electrochem.Soc.,* 137 (2), 675-679, ISSN 0013-4651

Glezos, N.; Patsis, G.P.; Raptis, I. & Argitis, P. (1996). Application of a reaction-diffusion model for negative chemically amplified resists to determine electron-beam proximity correction parameter, *J.Vac.Sci..Technol*. B, 14(6), 4252-4256, ISSN 1071-1023

Greeneich, J.S. (1974). Time evolution of developed contours in PMMA electron resist, *J. Appl. Phys.,* 45, 5264-5268, ISSN 0021-8979

Grigorescu, A.E.; Krogt, M.C.v.d.; Hagen, C.W. & Kruit, P. (2007). 10 nm lines and spaces written in HSQ using EBL, *Microel. Engineering*, 84 (5-8), 822-824, ISSN 0167-9317

Hatzakis M. (1998). PMMA co-polymers as high sensitivity electron resist, J.Vac. Sci. Technol. B, 16 (6), 1984-1988, ISSN 0022-5355

Hatzakis, M.; Ting, C.H. & Viswanathan, N.S. (1974). Fundamental aspects of electron beam exposure of polymeric resist system, *Proceed. of 6-th Int. Conf. on Electron and*

Ion Beam Science and Technol. Electrochem Soc., Princeton, N.J., 542-579, ISSN 0013-4651

Ishii, T.; Nozawa, H.; Tamamura, T. & Ozawa, A.. (1997). C_{60}-incorporated nanocomposite resist system for practical nanometer pattern fabrication, *Journal Vac.Sci.Technol*.B, 15 (6), 2570-2574, ISSN 1071-1023

Jamieson, A.T.; Willson, C.G.; Hsu, Y. & Brodie, A.D. (2002). HSQ bilayer resist process for low voltage EBL, *Proc. SPIE 4690*, 1171-1179, ISSN 0167-9317

Jewett, R.E.; Hagouel, P.I.; Neureuther A.R. & Duzer T.Van. (1977). Line profile resist development simulation techniques, *Polymer Engineering and Sciences*, 17(6), 381-384, ISSN 0032-3888

Jones, E. & Paraszczak, J. (1981). Computer simulation of resist development of 3D images, IEEE Trans. on El.Devices ED-28, 12, 1544-1552, ISSN 0018-9383

Karapiperis, L.; Adesida, I.; Lee, C.A. & Wolf, E.D. (1981). Ion beam exposure profiles in PMMA computer simulation, *J.Vac.Sci.Technol*. 19 (4), 1259-1263, ISSN 0022-5355

Kim, D.J.; Oldham W.G. & Neuteuther A.R. (1984). Development of positive resist, I*EEE Trans. Electr.Devices,* vol. ED-31, 12, 1730-1736, ISSN 0018-9383

Kishkovich, O.; Kinkead, D.; Higley, .; Kerwin, R. & Piatt, J. (1999). Real-time methodologies for monitoring airborne molecular contamination in modern DUV photolithography facilities, *Proc. SPIE*, 3677 (I), 348-376**,** ISSN 0277-786X

Mack, C. (1987). Development of positive photoresist, *J.Electrochemical Soc*., 134 (1), 148-152, ISSN 0013-4651

Matsuzawa, T. (1985). 3D photoresist image simulation, *IEEE El.Devices Letters,* EDL-6, 8, 416-418, ISSN 0193-8576

Merhari, L.; Gonsalves, K.E.; Hu, Y.; He, W.; Huang, W.S.; Angelopoulous, M.; Bruenger, W.H.; Dziong, C. & Torkler, M. (2002). Nanocomposite resist system for next generation lithography, *Microel.Engineering,* 63 (4), 391-402, ISSN 0167-9317

Millard, L.; Cunde, G.; Tedeso, S.; Dal'zotto, B. & Voucher, J. (2002). HSQ hybrid lithography for 20 nm CMOS device development, *Microel. Eng.* 62-63, 755-761, ISSN 0167-9317

Mladenov, G.M. & Emmoth, B. (1981). PMMA Sensitivity Variation versus the Electronic Stopping Power at Ion Lithography Exposure, *Appl. Phys. Letters*, 38 (12), 1000-1002, ISSN 0003-6951

Mladenov, G.M.; Braun, M.; Emmoth, B. & Biersack, J.P. (1985). Ion Beam Impact and Penetration of Polymethil Methacrylate, *J.Appl.Physics,* 58(7), 2534-2538, ISSN 0021-8979

Mladenov G. & Seyfarth H. (1986). General problems of microlithography, *Vacuum,* 36, 649-653, ISSN 0042-207X

Mladenov, G.; Dimitrova, R. & Vutova, K. (1987). Numerical modeling of penetration of accelerated electrons in materials, *Bulg.Physical Journal,* 14 (5), 446-456, ISSN 0584-0279

Mladenov, G. & Vutova, K. (2002). Computer simulation of exposure and development in EBL and IBL. *Proceedings of St.-Petersburg Electro-technical University, Solid State Physics and Electronics*, 1, pp.133-173, ISBN 020617, St.-Petersburg, Russia, April 2002, ed. B. A.Kalinikos, publisher SPbGETU LETI

Moreau, W.; Merrit, D.; Moyer, W.; Hatzakis M.; Johnson, D. & Pederson, L. (1979). Speed enhancement of PMMA resist, *J.Vac.Sci.Technol.* B, 16(6), 1989-1991, ISSN 0734-211X

Namatsu, H. (2001). Supercritical resist drying for isolated nanoline formation, *Journal Vacuum Sci. Technology* B, 19 (6), 2709-2712, ISSN 1071-1023

Namatsu, H.; Yamaguchi, T.; Nagase, N.; Yamazaki, K. & Kurihara, K. (1998). Resist Materials Providing Small Line-Edge Roughness, *Microel. Engineering,* 41-42, 331-334, ISSN 0167-9317

Neureuther, A.R.; Kyser, D.F. & Ting, C.H. (1979). Electron beam resist edge profile simulation, *IEEE Trans. on electron devices* ED-26, (4), 686-693, ISSN 0018-9383

Novembre, A.E. & Munzel, N. (1996). The EB and X-ray lithographic performance of the high resolution CAMP and ARCH family of CARs, *Microel.Engineering,* 32, 229-236, ISSN 0167-9317

Ryssel, H.; Haberger, K. & Kranz, H. (1991). Ion beam sensitivity of polymer resists*, J.Vac. Sci. Technol*., 19 (4), 1358-1362, ISSN 0734-2101

Sekiguchi, A.; Tajima, K.; Matsuzawa, T. & Kurihara, M. (2001). System for measurement of the development parameters of electron beam resists, *Electronics and Communications in Japan, Part II*, 84 (4), 16-25**,** ISSN 8756-663X

Vutova, K. & Mladenov, G. (1991). Absorbed energy distribution in electron lithography of simple patterns, *J. Inform. Recording Materials*, 19 (4), 271-282, ISSN 1025-6008

Vutova, K. & Mladenov, G. (1994). Modelling of exposure and development processes in electron and ion lithography. *Modelling and Simulation in Materials Science and Engineering*, 2, 239-254, ISSN 0965-0393

Vutova, K. & Mladenov, G. (2001). Sensitivity, contrast and development process in electron and ion lithography. *Microelectr. Eng*., 57-58, 349-353, ISSN 0167-9317

Vutova, K. & Mladenov, G. (2008). Computer simulation of micro- and nano-structures at electron and ion lithography. *Journal of optoelectronics and advanced materials*, 10 (1), 91-97, ISSN 1454-4164

(a) Vutova, K.; Koleva, E.; Mladenov, G. & Kostic, I. (2009). Some peculiarities of resist-profile simulation for positive-tone chemically amplified resists in electron beam lithography. *J.Vac.Sci.Technol. B,* 27 (1), 52-57, ISSN 1071-1023

(b) Vutova, K.; Koleva, E.; Mladenov, G.; Kostic, I.; Tanaka, T. & Kawabata. K. (2009). A simulation model for CAR CAMP6. *Microel. Eng.*, 86 (4-6), 714-717, ISSN 0167-9317

Wahlbrink,T.; Kupper, Dan.; Georgiev, Y.; Boten, J.; Moeler, M.; Kupper, Dav.Lemme, M.C. & Kurz, H. (2006). Supercritical drying process for high-aspect-ratio HSQ nano-structure, *Microel. Engineering,* 83 (4-9), 1124-1127, ISSN 0167-9317

Weiβ M.; Binder, H. & Schwalm, R. (1995). Modeling and simulation of a chemically amplified DUV resists, *Microelectronic Engineering,* 27 (1-4), 405-408, ISSN 0167-9317

Word, M.J.; Adesida, I. & Berger, P.R. (2003). Nanometer-period gratings in HSQ fabricated by EBL, *Rapid commun. in Journ.Vac.Sci.Technol.* B, 21 (6), L12-L15, ISSN 1071-1023

Yang, J.K.W. & Berggren, K. (2007). Using high-contrast salty development of HSQ for sub-10-nm half-pitch lithography, *J.Vac.Sci.Technol*. B, 25 (6), 2025-2029, ISSN 1071-1023

Yasin, S.; Hasko, D.G. & Ahmed, H. (2002). Comparison of MIBK/IPA and water/IPA as PMMA developers for EB nanolithography, *Microel. Eng.,* 61-62, 745-753, ISSN 0167-9317

Yasin, S.; Khalid, M.N. & Hasko, D.G. (2004). Reduction in Roughness of Resist Features in PMMA due to the Absence of a Rinse, *Jpn.J.Appl.Phys.*,43,6984-6987, ISSN 0021-4922

Yen, A. (2002). Erratum: (Optical Microlithography XV), *Proc. SPIE*, v.4691 II, 1769-1770, ISSN 0167-9317

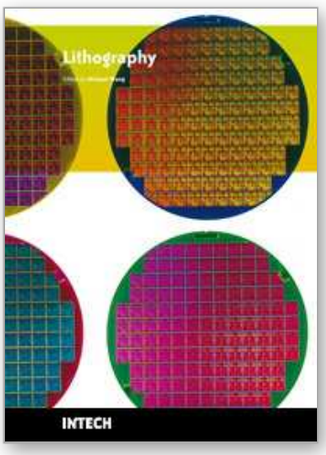

Lithography

Edited by Michael Wang

ISBN 978-953-307-064-3

Hard cover, 656 pages

Publisher InTech

Published online 01, February, 2010

Published in print edition February, 2010

Lithography, the fundamental fabrication process of semiconductor devices, plays a critical role in micro- and nano-fabrications and the revolution in high density integrated circuits. This book is the result of inspirations and contributions from many researchers worldwide. Although the inclusion of the book chapters may not be a complete representation of all lithographic arts, it does represent a good collection of contributions in this field. We hope readers will enjoy reading the book as much as we have enjoyed bringing it together. We would like to thank all contributors and authors of this book.

InTech Europe

University Campus STeP Ri

Slavka Krautzeka 83/A

51000 Rijeka, Croatia

Phone: +385 (51) 770 447

Fax: +385 (51) 686 166

www.intechopen.com

InTech China

Unit 405, Office Block, Hotel Equatorial Shanghai

No.65, Yan An Road (West), Shanghai, 200040, China

中国上海市延安西路65号上海国际贵都大饭店办公楼405单元

Phone: +86-21-62489820

Fax: +86-21-62489821

IntechOpen